Estimation of atmospheric instability during dust storms: A case study of Dalanzadgad station, Mongolian Gobi

Tergel Shijirtuya[*], Gan-Erdene Tsengel[**]

[*]Research Division of General Circulation and Long-Range Prediction, Information and Research Institute of Meteorology, Hydrology and Environment
[**]Research Division of Surface Water, Information and Research Institute of Meteorology, Hydrology and Environment

DOI: 10.29322/IJSRP.12.09.2022.p12952
http://dx.doi.org/10.29322/IJSRP.12.09.2022.p12952

Paper Received Date: 15th August 2022
Paper Acceptance Date: 15th September 2022
Paper Publication Date: 26th September 2022

Abstract- Although many scientists have focused on the spatiotemporal distribution of dust storm in Mongolia, there are a few studies have considered physical process.
The atmospheric stability parameters such as Brunt-Vaisala frequency (N), Gradient Richardson Number (Ri) and Eady Growth Rate (σ_E) were evaluated on 3 different cases of heavy dust storms which are occurred from March to May 2020, covered almost all over Mongolia, using reanalysis data produced by European Centre for Medium-Range Weather Forecasts and radiosonde data from "Dalanzadgad" aerological station in Dalanzadgad, Umnugovi. Differential equations of N, Ri and σ_E are solved using finite difference method.
The results of the study reveal that the distribution of dust storm represented well by both Ri and σ_E stability parameters , while linear relationship between dust storm and N as well as the buoyancy component of Ri was not found.

Key words - atmospheric instability, baroclinic stability, dynamic unstable, static stable, wind shear

I. INTRODUCTION

A dust storm is a phenomenon in which dust is released into the atmosphere under the influence of strong winds and then moves to a certain space. Dust storm highly depends on atmospheric circulation system, meteorological parameters near the ground surface and soil properties (Goudie, 1983; Qian et al., 2002; Wang et al., 2004; Shao and Dong, 2006). When the cyclone becomes active near the ground surface related with upper level through, pressure gradient increases and strong winds are created. Dust storms are generated by these strong winds, from the Gobi Desert (Chen et al, 1991; Kurosaki and Mikami, 2003; Jugder et al, 2004, Zhao L. and Zhao S., 2006). Researchers described the threshold wind speeds when dusts are released exceed 6.0 m/s or more over the Mongolian Gobi Desert region (Natsagdorj et al., 2003; Kurosaki and Mikami, 2007; Jugder et al., 2014).

Dust particles generated by dust storm from the Gobi Desert region of southern Mongolia and northern China (inner Mongolian autonomous region) release into the atmosphere and transport over the East Asian region, such as Korea and Japan, even can reach to the western coast of US through the pacific (Husar et al, 2001; Shao and Wang, 2003; Tsedendamba et al, 2019). Some negative impacts such as lost and deaths, delays in pasture for livestock, closures of roads, delays of flights occur during severe dust storms, due to the reduction of visibility (Natsagdorj et al, 2003; Shao and Wang, 2003, Jugder and Shinoda, 2011). Atmospheric windblown dust presents serious risk for human health, especially for the respiratory and cardiovascular system (Perkins 2001, Zhang et al., 2016; Goudie, 2020).

In Mongolia, about 60 percent of annual dust storms occur in the spring time, and around 65-91 percent occurs in a daytime and 9-35 percent observes in the nighttime, while dust storms extend an average of 3-6 hours per day (Natsagdorj et al., 2003). Natsagdorj et al described that dust storm mostly occurs when relative humidity is less than 40%. According to the observation data of more than 30 meteorological stations in Mongolia, from 1960 to 2013, the number of days with dust storm is increased almost 3 times (MARCC, 2014).

In general, dust storm studies mostly tend to estimate the synoptic process during a dust storm, weather and climatic parameters, soil surface properties and wind speed thresholds for dusts (Shinoda et al., 2010; Jugder and Shinoda, 2011; Ishizuka et al., 2012; Jugder et

al., 2014). A few surveys (Lanigan et al., 2016) calculated an atmospheric stability during dust storm is one of the reasons to do this study.

The main objective of this study is to calculate an atmospheric stability during dust storm period in spring time, over Mongolia.

II. DATA USED

In this study, we used the radiosonde data which measured at 00 UTC (local time: UTC+8) in the morning and 12 UTC in the evening from March to May 2020, at "Dalanzadgad" radiosonde station at Dalanzadgad (43°34'N 104°26'E), Umnugovi province, Mongolia. Figure 1 shows the location of "Dalanzadgad" radiosonde station.

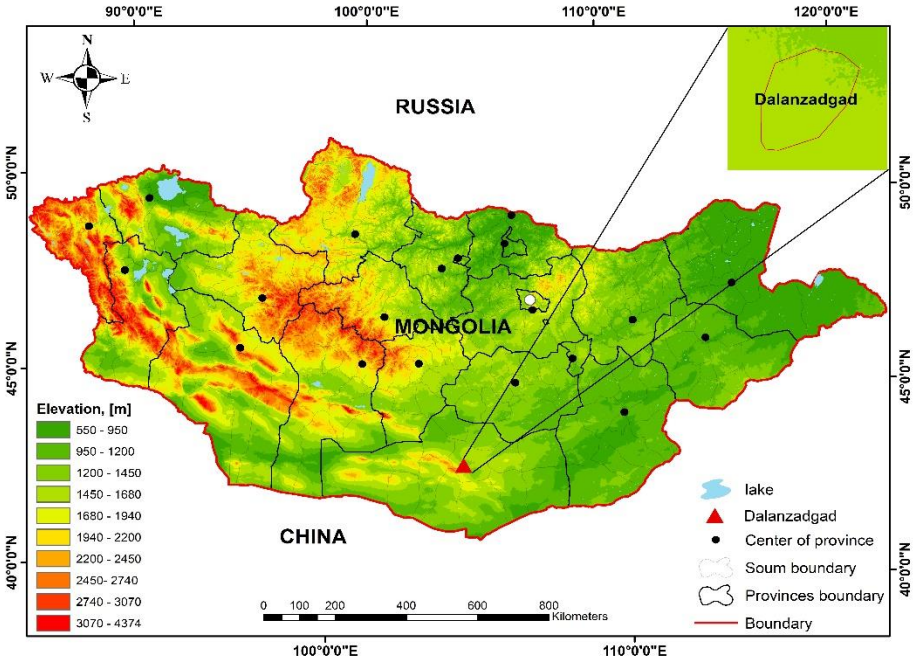

Figure 1. Elevation map of Mongolia

Dalanzadgad station is located in the southern part of Mongolia and is one of the four upper air stations in there. Of those four stations, only Dalanzadgad station is located in the Gobi Desert which has high frequency of dust storm (Natsagdorj et al., 2003). Therefore, we chose this station to calculate the stability parameters during dust storm. Interpolation was made to convert measured pressure values to standard levels.

Table 1. Description of GTS1 Radiosonde

	Pressure	**Temperature**	**Humidity**
Range	1060hPa – 5hPa	(-90)°C – (+50)°C	0% – 100%
Resolution	0.1hPa	0.1°C	1%

Also, we used ECMWF reanalysis (ERA5) pressure level data (Hersbach et al, 2018) for the areas where radiosonde launch is not performed (Table 1). In this study, we used air temperature, humidity and wind speed values at 16 layers from 850 to 100 hPa pressure level from the ERA5 reanalysis data, for each of the above periods.

Table 2. Description of ERA5

Data type	**Grid**
Horizontal resolution	0.25°x0.25°
Vertical resolution	37 pressure level
Temporal resolution	hourly

Source: https://www.ecmwf.int/

III. METHODOLOGY

Strong dust storm occurred on March 24, April 15, May 15, 2020, over the most part of Mongolia. We calculated the atmospheric stability parameters on these days.

Atmospheric instability

Instability occurs variously in the atmospheric motion. Static or thermal instability due to the vertical distribution of air temperature occurs when it is greater than dry adiabatic temperature gradient in unsaturated air and greater than moist adiabatic temperature gradient in the saturated air (Holton, 2004). Such kind of instability can be defined by Brunt-Vaisala frequency which is expressed as follows

$$N = \left(\frac{g}{\theta_{va}}\frac{\partial\theta_{va}}{\partial z}\right)^{1/2} \quad \text{(I)}$$

Where $g = 9.81$ m/s^2 is gravitational acceleration, θ_{va} is the ambient virtual potential temperature, and $\partial\theta_{va}/\partial z$ is the vertical gradient of the ambient virtual potential temperature. When N is equal to or greater than zero, the atmosphere is stable, while less than zero is considered to be in an unstable state (Holton, 2004).

Hydrodynamic instability is caused by the uneven distribution of air flow velocities. The theoretical application of hydrodynamic instability can do numeric evaluation of the mechanism of numerical and other characteristics on development stages and further evolutions of atmospheric vorticities and waves (Stull, 1988). One form of hydrodynamic instability which caused by the interaction of Coriolis force and buoyancy is baroclinic instability, expressed in Richardson number.

$$Ri = \frac{\frac{g}{T_V}\frac{\partial\theta_v}{\partial z}}{\left(\frac{\partial U}{\partial z}\right)^2 + \left(\frac{\partial V}{\partial z}\right)^2} \quad \text{(II)}$$

Where T_V is virtual absolute temperature, θ_v is virtual potential temperature, z is height, U and V are wind components toward the east and north. Theoretically, air is dynamic unstable when the Gradient Richardson number (Ri) is less than 0.25 (Miles, 1961; Howard, 1961), and turbulent motion predominates (Stull, 1988).

$\frac{g}{T_V}\frac{\partial\theta_v}{\partial z}$ in equation (II) is buoyancy of air mass, $\left(\frac{\partial U}{\partial z}\right)^2 + \left(\frac{\partial V}{\partial z}\right)^2$ is shear between vertical layers of air flow. Since, $\frac{g}{T_V}\frac{\partial\theta_v}{\partial z}$ is called buoyancy and $\left(\frac{\partial U}{\partial z}\right)^2 + \left(\frac{\partial V}{\partial z}\right)^2$ is called wind shear.

One another parameter which can express the baroclinic instability is Eady Growth Rate.

$$\sigma_E = 0.3098\frac{|f|\left|\frac{\partial U(z)}{\partial z}\right|}{N} \quad \text{(III)}$$

Where f is Coriolis parameter ($f = 2\Omega sin\varphi$, $\Omega = 7.292 \times 10^{-5}$ rad/s is the angular speed of the earth, φ is the latitude), $U(z)$ is vertical profile of the eastward wind component and N is Brunt-Vaisala frequency. σ_E has the advantage of representing system development in the environment as well as atmospheric instability (Simmonds and Lim, 2008).

Generally, atmospheric instability occurs when the wind is moving through the horizontal and vertical dimension along with the horizontal inhomogeneity of air temperature. As a result of hydrodynamic instability, synoptic scale cyclone vortices and atmospheric wave motions cause various kind of weather phenomena (Natsagdorj, 2017).

Using These instability parameters (N, Ri, σ_E), calculations were made for the actual observation (radiosonde) and ERA5 reanalysis data for each of the above three periods.

IV. RESULTS

To determine the atmospheric stability, the solutions of equations (I), (II) and (III) described above were calculated on the days of dust storms using the finite difference method. In the calculation of stability along the vertical dimension of the atmosphere, we used radiosonde measurement data of "Dalanzadgad" upper air station in Dalanzadgad, Umnugovi province. The calculation of stability in the horizontal distribution was based on ERA5 reanalysis data with resolution of 0.25°x0.25°.

A. Vertical distribution of the atmospheric stability

Atmospheric stability parameters were calculated for each of the three cases which are mentioned above is divided into three stages: "before the dust storm", "during dust storm" and "after dust storm", using radiosonde data of "Dalanzadgad" station, and the results are shown in Tables 3, 4 and 5. Table 3 shows the period "before dust storm", Table 4 shows the period "during dust storm" and Table 5 shows the period "after dust storm", respectively.

The calculations were performed as described in the "Methodology" section, and the values of σ_E, N, buoyancy and wind shear were multiplied by 10^6, 10^2, 10^4 and 10^5, respectively to convert whole values.

As can be seen from the Table 3, the values of Ri are greater than 2 and N is greater than 0, which ensures that the atmosphere is hydrodynamically and statically stable on all the pressure levels. The value of σ_E which calculated by the average of the three cases of

dust storms is ranging between from 2 to 20, indicating that the atmosphere is in a static and hydrodynamic stable state before the event.

Table 3. Instability parameters calculated by radiosonde measurement data of the "Dalanzadgad" station (before dust storm period)

Pressure levels	σ_E	Ri	N	buoyancy	Wind Shear
850	19.14	1.50	1.61	2.96	32.83
825	5.80	11.96	1.31	1.81	2.74
800	18.28	1.50	0.90	0.81	10.65
775	16.05	1.50	0.90	0.81	5.61
750	14.54	2.61	1.01	1.13	3.93
700	6.62	7.83	1.04	1.20	2.02
650	10.77	6.52	0.96	1.04	2.82
600	8.71	14.66	0.88	0.91	3.58
550	6.66	14.04	0.84	0.82	2.53
500	5.23	25.15	1.00	1.03	0.53
400	5.07	27.23	0.98	0.96	0.48
300	2.40	84.67	1.04	1.13	0.13
250	3.45	129.82	1.78	3.22	0.72
200	2.52	142.14	2.17	4.71	0.61
150	2.32	320.40	2.07	4.31	0.34
100	3.44	49.99	1.92	3.68	0.79

As shown in Table 4, the value of Ri is between 0.04...0.09 at a pressure level of 850-800 hPa, which indicates that the atmosphere was in hydrodynamic unstable state, and the value of N is greater than 0, that the atmosphere exists under static stable state. The main reason to exist under the hydrodynamic unstable state is wind shear between the pressure layers. For the σ_E, greater than 100 at the pressure levels of 850 and 825 hPa, indicates the presence of baroclinic unstable conditions in the atmosphere, as well as the fact the system is in active development. Also, N was less than 0 during dust storm which occurred on 15th of May, and atmosphere was existing under the static unstable state, buoyancy was supported baroclinic unstable condition more or less, but relatively small in value. Since N was negative, σ_E was also negative, with an absolute value was greater than 100.

Table 4. Instability parameters calculated by radiosonde measurement data of the "Dalanzadgad" station (during dust storm)

Pressure levels	σ_E	Ri	N	buoyancy	Wind Shear
850	104.89	0.04	0.62	0.91	117.92
825	128.51	0.09	0.44	0.47	45.72
800	83.67	0.67	0.35	0.22	35.07
775	70.99	0.38	0.35	0.25	6.52
750	21.66	0.32	0.54	0.30	10.70
700	19.66	0.83	0.79	0.68	9.20
650	13.40	1.39	1.00	1.14	8.01
600	27.14	4.83	0.98	1.10	13.64
550	22.27	6.90	1.00	1.07	4.76
500	13.47	2.82	1.14	1.32	5.73
400	9.94	4.91	1.11	1.25	2.98
300	5.36	29.49	1.14	1.31	1.47
250	8.75	23.03	1.86	3.47	7.31
200	4.29	18.79	2.16	4.68	3.33
150	2.08	180.72	2.06	4.23	0.24

100	3.05	91.70	1.92	3.70	0.45

In the Table 5, atmospheric stability parameters are same as the period before dust storm. A difference is σ_E couldn't get enough value even atmosphere is in hydrodynamic unstable state as a result of wind shear was more at a pressure level of 850 hPa. In other words, it indicates the atmospheric process was going shut down.

Table 5. Instability parameters calculated by radiosonde measurement data of the "Dalanzadgad" station (after dust storm period)

Pressure levels	σ_E	Ri	N	buoyancy	Wind Shear
850	49.25	0.18	1.48	2.31	199.38
825	28.19	1.07	1.31	1.74	154.16
800	14.03	4.47	1.10	1.23	12.55
775	21.38	4.23	1.36	1.92	41.36
750	21.75	2.76	1.48	2.22	21.30
700	16.19	1.73	1.45	2.19	12.42
650	9.84	7.40	1.24	1.65	2.63
600	5.61	2.89	1.23	1.52	21.87
550	30.37	2.10	1.45	2.12	147.32
500	31.06	9.55	1.19	1.42	53.03
400	3.02	6.75	1.04	1.10	2.45
300	22.43	18.87	1.15	1.34	18.69
250	14.89	12.61	1.67	2.83	11.04
200	3.68	29.23	2.08	4.34	3.92
150	5.48	22.65	2.11	4.44	2.69
100	2.42	173.39	1.98	3.95	0.43

As shown in Table 5, the value of Ri is less than 0.25 at a pressure level of 850 hPa, which is dynamically unstable. Ri is a parameter which depends on buoyancy and wind shear. However, according to this study, the numerical value of buoyancy component of hydrodynamic instability was around 0.2-3.0 at each stage of the three cases. Theoretically, since the time we have chosen is spring, the buoyancy may have little effect on hydrodynamic instability in absolute terms due to the fact that the soil surface is not sufficiently warm enough to allow air mass buoyancy to occur rapidly.

B. Horizontal distribution of the atmospheric stability

According to the observational data provided by "National Agency of Meteorology and Environment Monitoring", dust storm was occurred on 24th March, 2020 over the most of the central part of Mongolia, and during this period wind speed reached 10-18 m/s. The disaster lasted from 09:48 to 19:11 (local time: UTC+8) in the central part, and the spatial distribution of the coverage period is shown in Figure 2.

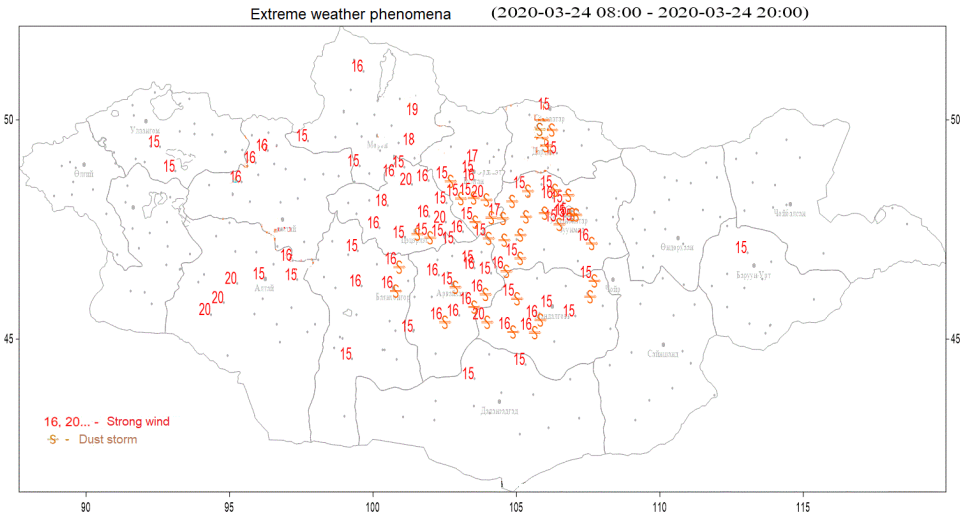

Fig. 2. Spatial distribution of wind speed (m/s) and dust storm over Mongolia, on 24th March 2020 (by the real observation data from 08:00 to 20:00)

Figure 3 shows the spatial distribution of the mean value of σ_E and the smallest value of Ri calculated by ERA5 reanalysis data, during from 08:00 to 20:00 on 24th March 2020, at a pressure level of 850 hPa. Both the figures drawn by actual observation (Fig. 2) and reanalysis data (Fig. 3) are similar for spatial distribution. While, atmospheric dynamic and baroclinic instability were relatively high on the east side of Khentei mountain and it is a reason to occur snow storm in this area.

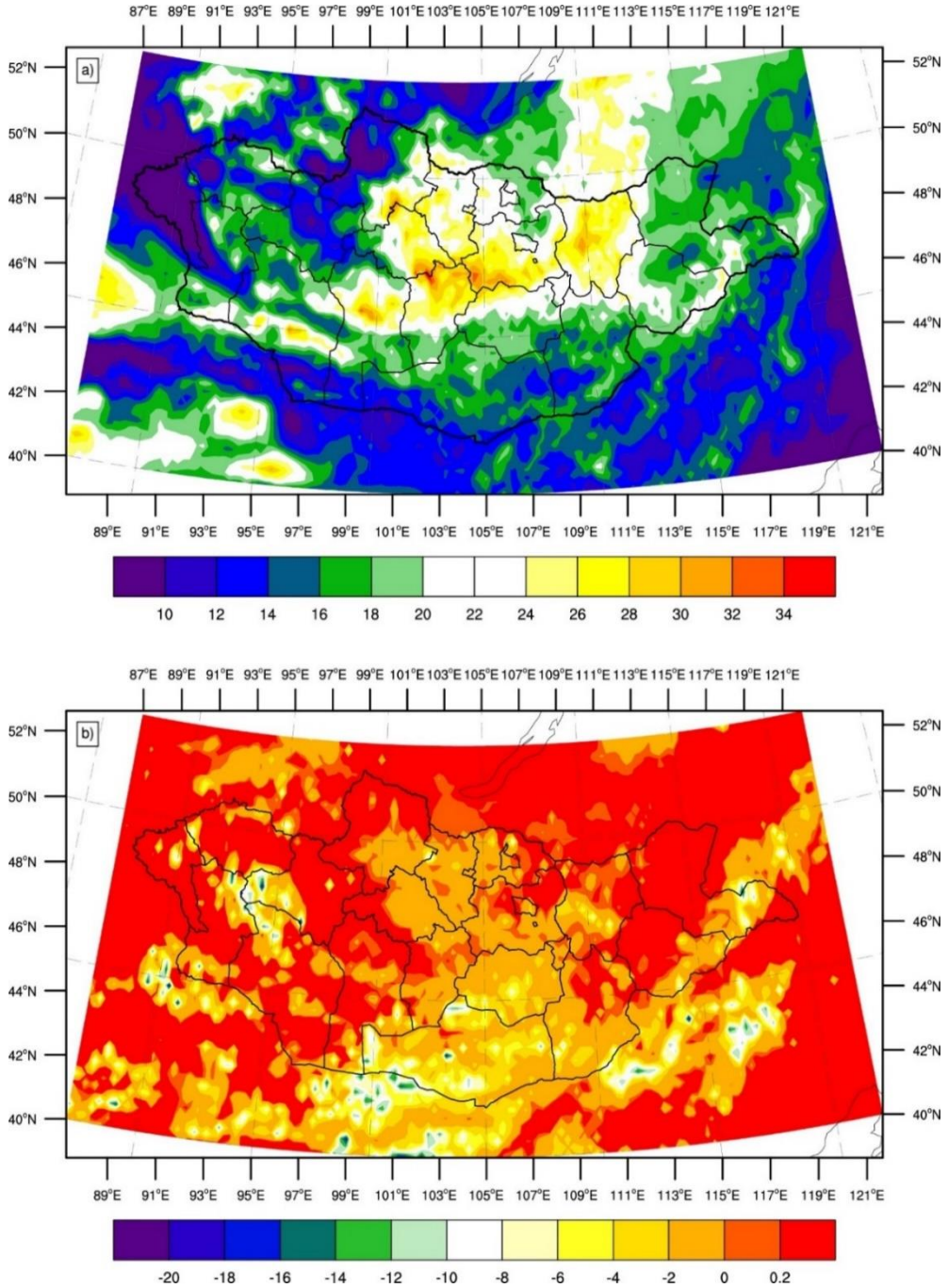

Fig. 3. Spatial distribution of (a) the mean value of σ_E and (b) the smallest value of Ri calculated by ERA5 reanalysis data (from 08:00 to 20:00, on 24th March 2020)

On 15th April 2020, wind speed reached 14-18 m/s in the southern east part of Mongolia. Figure 4 shows the wind speed distribution during this period. In addition, the calculation of stability values using the ERA5 reanalysis data are shown in Figure 5. It looks similar in terms of spatial distribution as before. In particular, the distribution map of the mean value of σ_E calculated by the reanalysis data clearly shows the dust storm process.

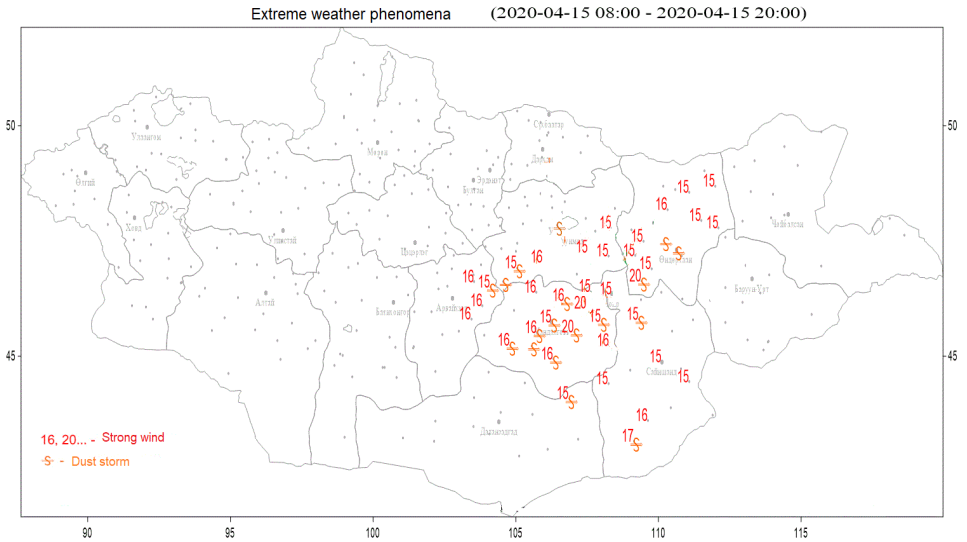

Fig. 4. Spatial distribution of wind speed (m/s) and dust storm over Mongolia, 15th April 2020 (by the real observation data from 08:00 to 20:00)

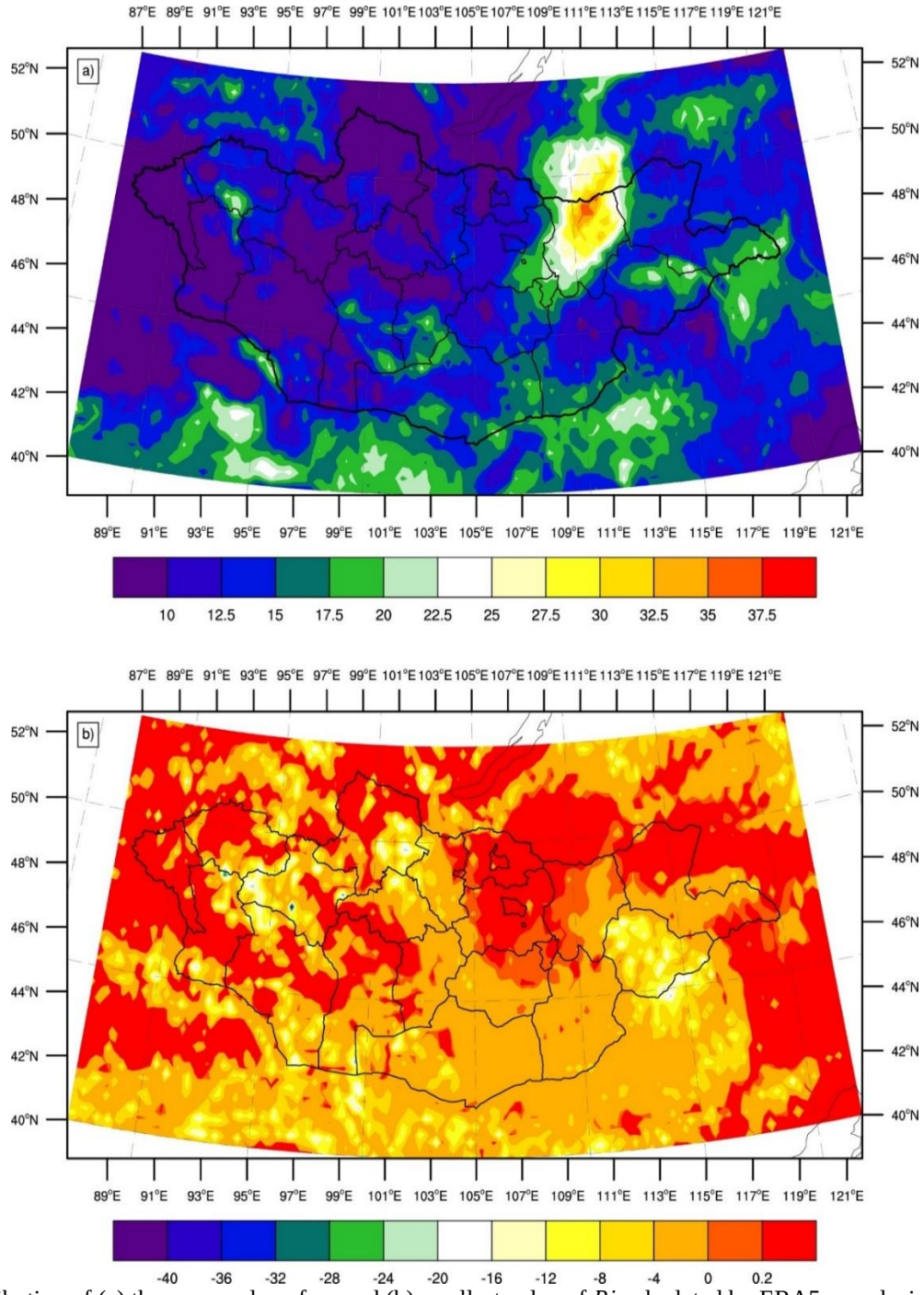

Fig. 5. Spatial distribution of (a) the mean value of σ_E and (b) smallest value of Ri calculated by ERA5 reanalysis data (from 08:00 to 20:00, on 15th April 2020)

Also, on 15th May 2020, wind speed reached 10–20 m/s in the most parts of the central, eastern and southern part of Mongolia, causing dust storm that reached disaster level. Figure 6 shows the spatial distribution of the actual observed wind speed during the process, and Figure 7 shows the distribution of the values of σ_E and Ri calculated by the reanalysis data. The distribution maps of σ_E and Ri mapped by ERA5 reanalysis data show the spatially detailed snow and dust storm areas. The results of this study show that if we have a more accurate spatial analysis data, we can use it to calculate σ_E and calculate the spatial distribution of dust storms in areas not known for observation.

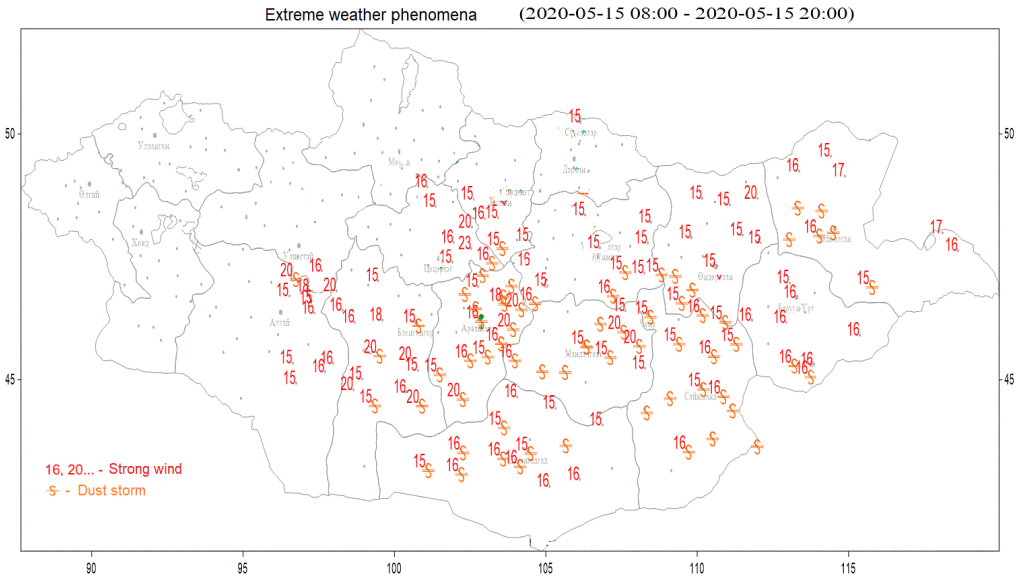

Fig. 6. Spatial distribution of wind speed (m/s) and dust storm over Mongolia, 15th May 2020 (by the real observation data from 08:00 to 20:00)

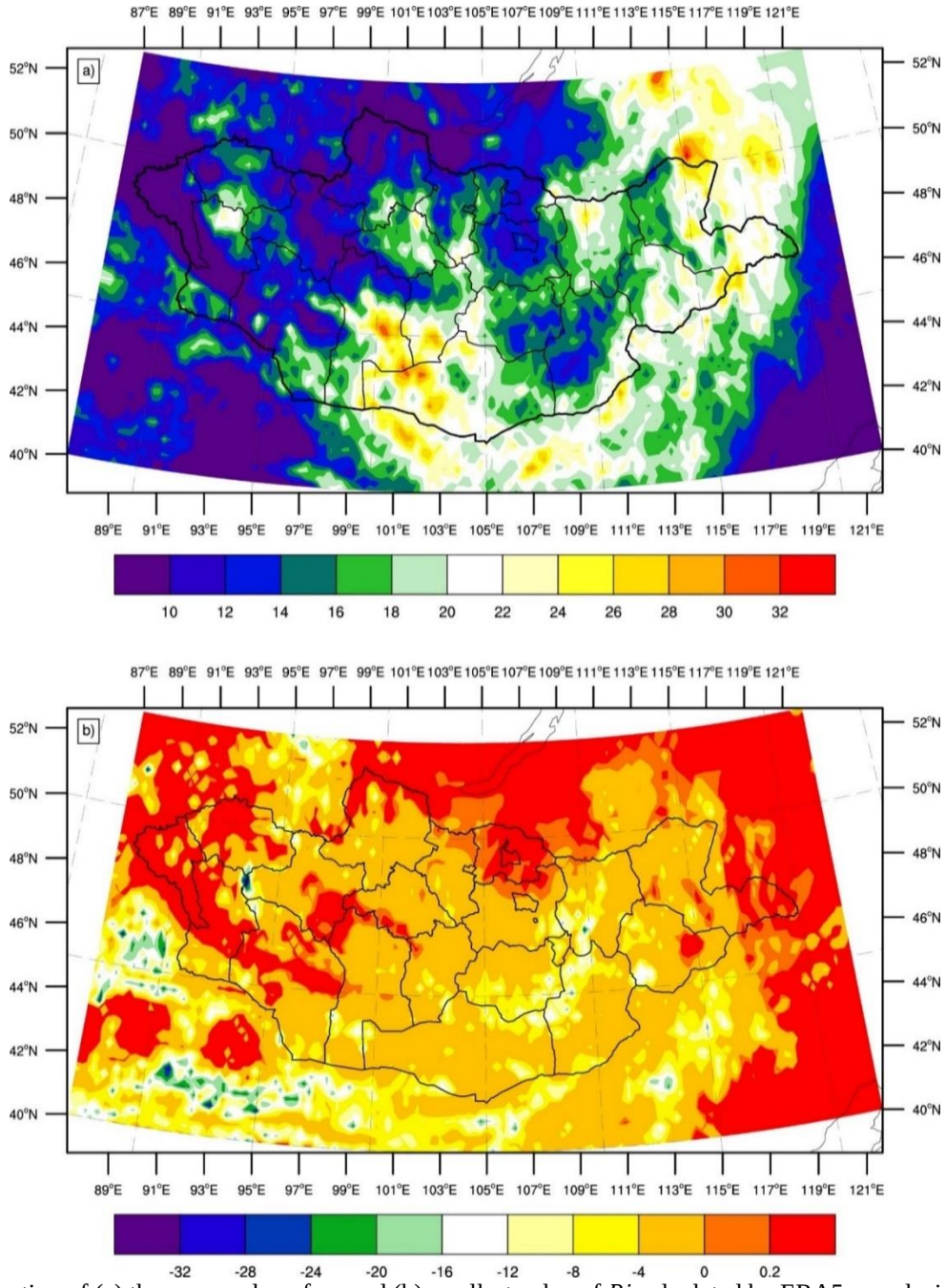

Fig. 7. Spatial distribution of (a) the mean value of σ_E and (b) smallest value of Ri calculated by ERA5 reanalysis data (from 08:00 to 20:00, on 15th May 2020)

V. CONCLUSIONS

In this study, we calculated the atmospheric stability parameters on the three cases (24th March, 15th April and 15th May 2020) of strong dust storm covered over the most area of Mongolia. The following conclusions are drawn from the results of the calculation of the atmospheric static and hydrodynamic instability parameters for each stage of dust storm.

The parameters Ri and N which represent the atmospheric stability calculated in this study, are 0.04...0.09 and 0.44...0.62 at the atmospheric lower layers of 850-825 hPa, respectively, during dust storms means that they reached the threshold value which indicates the atmospheric instability and we consider that the parameters can determine the dynamic and static state of the atmosphere, theoretically.

Atmosphere is in static unstable state doesn't have a major effect on dynamic instability, but rather supports it. In other words, dynamic instability depends on wind shear, even atmosphere is in any state of static.

The horizontal distribution of σ_E and Ri calculated by ERA5 reanalysis data coincides with the actual observation data, indicating that it is possible to calculate the dust storm distribution using these parameters.

ACKNOWLEDGMENT

This study was funded by a research grant from the Green Climate Fund's "Capacity Building for National Climate Change Planning" project implemented by the Ministry of Nature, Environment and Tourism and the United Nations Environment Program.

REFERENCES

[1] S. Chen, Y. Kuo, P. Zhang, and Q. Bai, "Synoptic climatology of cyclogenesis over East Asia, 1958-1987", *Monthly Weather Review*, vol. 119(6), 1991, pp. 1407-1418.

[2] A. S. Goudie, "Dust storms in space and time", *Progress in Physical Geography*, vol. **7**(4), 1983, pp. 502-530.

[3] A. S. Goudie, "Dust Storms and Human Health", *Extreme Weather Events and Human Health*, Springer, Cham, 2020, pp. 13-24.

[4] H. Hersbach, C. Peubey, A. Simmons, P. Poli, D. Dee, and P. Berrisford, *ERA report series*, 2018.

[5] J. R. Holton, *Introduction to Dynamic Meteorology*. 4th Edition, Elsevier, Amsterdam, 2004, pp. 535.

[6] L. N. Howard, "Note on a paper of John W. Miles", *Journal of Fluid Mechanics*, vol. 10(4), 1961, pp. 509-512.

[7] R. B. Husar, D. M. Tratt, B. A. Schichtel, S. R. Falke, F. Li, D. Jaffe, S. Gasso, T. Gill, N. S. Laulainen, F. Lu, and M. C. Reheis, "Asian dust events of April 1998", *Journal of Geophysical Research: Atmospheres*, vol. 106(D16), 2001, pp. 18317-18330.

[8] M. Ishizuka, M. Mikami, Y. Yamada, R. Kimura, Y. Kurosaki, D. Jugder, B. Gantsetseg, Y. Cheng, and M. Shinoda, "Does ground surface soil aggregation affect transition of the wind speed threshold for saltation and dust emission?", *Science Online Letters on the Atmosphere (SOLA)*, vol. 8, 2012, pp. 129-132.

[9] D. Jugder, Y. S. Chung, and A. Batbold, "Cyclogenesis over the territory of Mongolia during 1999-2002", *Journal of the Korean Meteorological Society*, vol. 40, 2004, pp. 293-303.

[10] D. Jugder, and M. Shinoda, "Intensity of a dust storm in Mongolia during 29-31 March 2007", *Online Journal of the Science Online Letters on the Atmosphere (SOLA)*, vol. **7**A, 2011, pp. 029-031.

[11] D. Jugder, M. Shinoda, R. Kimura, A. Batbold, D. Amarjargal, "Quantitative analysis on windblown dust concentrations of PM10 (PM2.5) during dust events in Mongolia", *Journal of the Aeolian Research*, vol. 14, 2014, pp. 3-13.

[12] Y. Kurosaki, and M. Mikami, "Recent frequent dust events and their relation to surface wind in East Asia", *Geophysical Research Letters*, vol. 30(14), 2003, pp. 1736.

[13] Y. Kurosaki, and M. Mikami, "Threshold wind speed for dust emission in east Asia and its seasonal variations", *Journal of Geophysical Research: Atmospheres*, vol. 112(D17), 2007, pp. 202.

[14] D. Lanigan, J. Stout and W. Anderson, "Atmospheric stability and diurnal patterns of aeolian saltation on the Llano Estacado", *Aeolian Research*, vol. 21, 2016, pp. 131-137.

[15] R. S. Lindzen, F. Brian, "A simple approximate result for the maximum growth rate of baroclinic instabilities", *Journal of the Atmospheric Sciences*, vol. 37, 1980, pp. 1648-1654.

[16] J. W. Miles, "On the stability of heterogeneous shear flows", *Journal of Fluid Mechanics*, vol. 10(4), 1961, pp. 496-508.

[17] Ministry of Environment and Green Development, *Mongolia second assessment report on climate change*, 2014.

[18] L. Natsagdorj, D. Jugder, and Y. S. Chung, "Analysis of dust storms observed in Mongolia during 1937-1999", *Journal of the Atmospheric Environment*, vol. 37, 2003, pp. 1401-1411.

[19] S. Perkins, "Dust, the thermostat", *Sci News*, vol. 160(13), 2001, pp. 200–201.

[20] W. Qian, L. Quan, and S. Shi, "Variations of the dust stroms in China and its climatic control", *Journal of Climate*, vol. 15(10), 2002, pp. 1216-1229.

[21] Y. Shao, and C. H. Dong, "A review on Asian dust storm climate, modeling and monitoring", *Global and Planetary Change*, vol. 52(1), 2006, pp. 1-22.

[22] Y. Shao, and J. Wang, "A climatology of Northeast Asian dust events", *Meteorologische Zeitschrift*, vol. 12(4), 2003, pp. 187-196.

[23] M. Shinoda, R. Kimura, M. Mikami, M. Tsubo, E. Nishihara, M. Ishizuka, Y. Yamada, E. Munkhtsetseg, D. Jugder, and Y. Kurosaki, "Characteristics of dust emission on the Mongolian steppe", The 2008 DUVEX Intensive Observational Period, *Science Online Letters on the Atmosphere (SOLA)*, vol. **6**, 2010, pp. 9-12.

[24] I. Simmonds, and E. Lim, "Biases in the calculation of Southern Hemisphere mean baroclinic eddy growth rate", *Geophysical Research Letters*, vol. 36(1), 2009, L01707.

[25] R. B. Stull, *An Introduction to Boundary Layer Meteorology*. Dordrecht: Kluwer Academic Publishers, 1988, pp. 666.

[26] P. Tsedendamba, D. Jugder, K. Baba, K. Hagiwara, J. Noda, K. Kawai, G. Sumiya, C. McCarthy, K. Kai, B. Hoshino, "Northeast Asian dust transport: A case study of a dust storm event from 28 March to 2 April 2012", *Atmosphere*, vol. 10, 2019, pp. 69.

[27] X. Wang, Z. Dong, J. Zhang, and L. Liu, "Modern dust storms in China: an overview", *Journal of Arid Environments*, vol. 58(4), 2004, pp. 559-574.

[28] X. Zhang, L. Zhao, D. Q. Tong, G. Wu, M. Dan, and B. Teng, "A systematic review of Global Desert dust and associated human health effects", *Atmosphere*, vol. **7**(12), 2016, pp. 158.

[29] L. Zhao, and S. Zhao, "Diagnosis and simulation of a rapidly developing cyclone related to a severe dust storm in East Asia", *Global and Planetary Change*, vol. 52(1-4), 2006, pp. 105-120.

AUTHORS

First Author – Tergel Shijirtuya, meteorology, tergel.shijir@gmail.com.
Second Author – Gan-Erdene Tsengel, hydrology, ttsg.0124@gmail.com.

Correspondence Author – Tergel Shijirtuya, tergel.shijir@gmail.com, teegiisemi@gmail.com, +976 89064608.